Cost-effective upgrade of the Dutch traction power network: Moving to Bi-directional and controllable 3 kV DC substations for improved performance

Panda, Nanda Kishor; Poikilidis, Michail ; Nguyen, Phuong H.

DOI
10.1049/els2.12084

Publication date
2023

Document Version
Final published version

Published in
IET Electrical Systems in Transportation

Received: 25 September 2022 | Revised: 15 February 2023 | Accepted: 23 April 2023

IET Electrical Systems in Transportation

DOI: 10.1049/els2.12084

The Institution of Engineering and Technology WILEY

CASE STUDY

Cost-effective upgrade of the Dutch traction power network: Moving to Bi-directional and controllable 3 kV DC substations for improved performance

Nanda Kishor Panda[1] | **Michail Poikilidis**[2] | **Phuong H. Nguyen**[3]

[1]The Faculty of Electrical Engineering, Mathematics and Computer Science, Delft University of Technology, Delft, The Netherlands

[2]Department of Energy Systems, DNV, Arnhem, The Netherlands

[3]The Faculty of Electrical Engineering, Eindhoven University of Technology, Eindhoven, The Netherlands

Correspondence

Nanda Kishor Panda.
Email: n.k.panda@tudelft.nl

Funding information

European Union's Horizon, Grant/Award Number: 864048; DNV Energy Systems

Abstract

Traction power networks can significantly influence a country's national grid due to their significant power consumption and numerous coupling points. To modernise the ageing Dutch traction power networks and enhance their impact on the utility grid, this study explores practical and cost-effective approaches for upgrading existing 1.5 kV DC traction substations (TS) in the Netherlands into 3 kV bi-directional DC TS. After evaluating the benefits of a 3 kV bi-directional DC, two novel topologies are proposed that re-use the existing substation's components and reduce the need for higher investments. These topologies incorporate parallel voltage source converters (VSCs) to recuperate braking energy from the DC grid and transfer it back to the AC grid. Furthermore, the study investigates additional use cases for the VSCs, including improving DC TS's reliability during faults, reducing harmonics through active power filtering, compensating for reactive power, and supporting the integration of renewable energy sources into the DC grid. A comprehensive control strategy for the VSCs is also proposed based on a thorough analysis of their working methodology and functional modes. The feasibility and effectiveness of the proposed solutions are validated through scenario analysis relevant to the Netherlands' traction network, utilising both a Simulink model and an Opal-RT real-time simulator. This study serves as a starting point for the various stakeholders of the Dutch traction network in their journey towards modernising the current traction power supply. It has the potential to serve as a reference for reusing existing railway infrastructures to provide ancillary services and support the energy transition.

KEYWORDS

power harmonic filters, PWM power convertors, rectifier substations, regenerative braking, traction

1 | INTRODUCTION

The rail transportation is one of the most efficient means of public transportation. Railway electrification in the 1800s was an important step in decarbonising the transportation sector, as electrification is crucial for the sustainability and efficiency of a country's transportation system. It leads to lower operating costs, reduced greenhouse gas emissions, and improved train performance, contributing to a more sustainable future for the transportation sector. In the future, electrified railways will be the only viable option for sustainability, making the interconnection between these systems and the national power grid

Abbreviations: APF, Active Power Filter; DRES, Distributed Renewable Energy Source; ESS, Energy Storage System; NS, Nederlandse Spoorwegen; PWM, Pulse Width Modulation; THD, Total Harmonic Distortion; TPS, Traction Power System; TS, Traction Substation; VSC, Voltage Source Converter.

crucial for the smooth operation of both the traction power networks and the grid. DC traction systems are popular throughout the European subcontinent, but the standard low voltage (LV) of DC traction networks limits the acceleration capabilities of locomotives and induces high line losses [1].

The Netherlands started its railways in 1908 using a 10 kV AC system, which later transitioned into a 1.5 kV DC system in 1922. The light-weighted and straightforward engines and infrastructures were the reasons for opting for a 1.5 kV traction power network [2]. Being Europe's busiest railway, the Dutch rail network is now operating at the top of its capacity. A forecast of a 14% increase in passenger kilometres between 2017 and 2023 has put its stakeholders searching for ways to upgrade the current railway networks [3]. Previous studies analysed alternatives like 1.5 kV ECO, 3 kV DC, and 15/25 kV AC systems to upgrade the existing rail network. For instance, in the 1.5 kV ECO system, the catenaries' voltage remains the same. Still, measures like optimising electrodynamic brakes and lowering transport resistance using coupled overhead lines in multi-track lines are taken to reduce electricity transportation losses and recover a larger part of the braking energy back to the DC grid. On the other hand, a 3 kV network will be more efficient due to lower line losses and the ability of trains to accelerate faster.

As the benefits of a 3 kV bidirectional Traction Power System (TPS) outweigh other methods, this paper proposes topologies for 3 kV bi-directional DC Traction Substation (TS) that can refurbish the existing 1.5 kV diode rectifier-based DC TS [4, 5]. With bidirectionality added, the 3 kV bidirectional TPS can increase the efficiency of braking energy recuperation and allow the direct integration of Distributed Renewable Energy Sources (DRESs) directly in the DC grid.

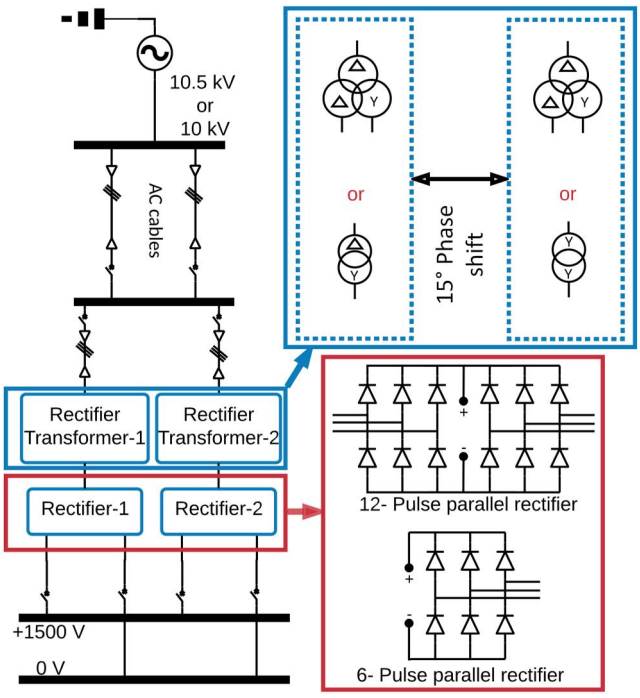

FIGURE 1 Electrical system layout of existing DC TSs present in the Netherlands highlighting the two different types of rectifier-transformer groups.

1.1 | Current system overview

The current Dutch railway traction system, used as a case study for this paper, is based on a 1.5 kV DC network with overhead connectors for catenary and rails for the return path, fed by multiple DC TS. Each DC TS primarily consists of two groups of transformer and diode-rectifier pairs with a mutual phase shift of 15°, connected to the medium voltage (MV) grid. The two rectifier groups help divide the total load, naturally eliminating specific harmonics and decreasing the output voltage ripple [6, 7]. Currently, two types of DC TS exist, which differ in their capacity and the types of transformers and diode rectifiers used. Figure 1 shows the schematic of the two different configurations used with their technical details provided in Table 1. Generally, the ideal no-load direct voltage and no-load phase-phase voltage ratio for different configurations of transformer and diode-rectifiers can be found in [8]. The current DC system is designed for a nominal voltage of 1.5 kV with a maximum current rating of 2600 A.

1.2 | Related works

Rail transportation is important to public transportation systems due to its ease, speed, and cost-effectiveness. DC railway networks are a popular choice in many parts of the world as their equipment is cheaper, lighter and more efficient than the AC traction counterpart [9]. 3 kV DC traction systems can be found in Belgium, Italy, Spain, Poland, Slovakia, South Africa, and Chile. Most of these places power the traction system

TABLE 1 Technical details of current DC traction substations configurations.

	Transformer					Diode rectifiers	
MV voltage	Type		Configuration	Capacity	Turns ratio	Configuration	DC output
10 kV	Two-winding	Trf-1	Δy11	2.5 MVA	10.6/1.376 kV	Two 6-pulse connected in parallel	12 pulse
		Trf-2	Yy0	2.5 MVA	11/1.326 kV		
10.5 kV	Three-winding	Trf-1	Zy0d −7.5°	5.4 MVA	10.75/1.326 kV	Two 12-pulse connected in parallel	24 pulse
		Trf-2	Zy0d +7.5°	5.4 MVA	10.75/1.326 kV		

using uncontrolled diode-rectifiers fed by transformers from the MV grid [10–12]. Like the Dutch traction system, most of the above TPSs contain either parallel 6-pulse, 12-pulse rectifiers, or series 12-pulse rectifiers [13, 14].

Series connection of LV rectifiers to achieve a higher output voltage has been seen to stabilise load voltage and introduce lesser alternative distortion voltage at the load side [15]. Series connected 6-pulse rectifiers are used in the railway lines east of Algeria [16]. To increase the distance between TS and limit the fault current, the Dallas Area Rapid Transit first introduced controlled rectifiers like reversible thyristor-controlled rectifiers in the early nineties [17]. TCRs can increase the size of substations by 15% but can decrease the payback time through savings from recuperation of the train's braking energy [18]. Though TCRs can have a quicker payback period of 2–2.5 years, improving overall efficiency by 60% using existing infrastructure, a clear trade-off must be made between Pulse Width Modulation (PWM) rectifiers using IGBTs and TCRs. Despite the higher cost and switching losses in high-power applications, IGBT-based converters can provide better controllability and more efficient recovery of braking energy [19, 20].

Efficiency in DC traction systems has always been a topic of interest for industrial and academic researchers, especially for unidirectional DC TSs, where the braking energy of trains is circulated within the DC grid, as in the case of the Netherlands' railway network [17]. Onboard or stationary wayside Energy Storage Systems (ESSs) are growing popular in urban transit systems to store the braking energy of vehicles using supercapacitors, batteries, or flywheels. Supercapacitor-type ESSs can be found in Mannheim (Germany), Innsbruck (Austria), Saragossa, Granada (Spain), and Paris (France), primarily for light rail or tram rail transportation networks [21]. Onboard ESS offer negligible line losses during braking energy recovery, reduces power peaks during vehicle acceleration, and helps stabilise supply voltage. Still, ESS need larger spaces in the locomotives; hence are preferred for newly designed vehicles rather than retrofitting them into existing locomotives [21].

Making DC TSs reversible has become one of the most favourable ways to utilise braking energy efficiently. Allowing excess energy from the DC grid to evacuate into the AC grid gives the natural exchange of regenerated energy among trains the highest priority level. In addition, certain reversible DC TSs can improve power quality on the AC side and stabilise supply voltage [17, 22].

1.3 | Research gaps and paper organisation

Researchers are focusing on developing future advanced and efficient railway transportation systems; however, limited research is being done to increase efficiency and convert existing unidirectional diode-based DC TS into reversible substations. Improving the existing system is essential due to the size, cost, and time requirements for constructing an entirely new system. Refurbishing existing TS will save considerable costs by reusing costly components like transformers and diode-rectifiers, also reducing the transition time to a new system; this paper proposes topologies to upgrade the existing 1.5 kV DC TS into 3 kV bi-directional TS. The upgraded voltage reduces line losses and can support a high-frequency train timetable by improving the train's acceleration and deceleration, while the bi-directionality efficiently recuperates braking energy. Particular attention has been given to exploring new applications of parallel voltage source converters (VSCs) that can offer ancillary services to the utility grid. This analysis can potentially make the modernisation of the existing 1.5 kV DC TS more attractive to the stakeholders of the traction power supply by uncovering new revenue streams.

2 | PROPOSED TOPOLOGIES

Two different topologies have been proposed for the existing DC traction systems. These topologies can be further divided into two parts: one that upgrades the DC traction voltage and another that makes the DC TS reversible. The proposed topologies aim to increase the efficiency of the DC TS. Using a higher 3 kV DC voltage, the copper loss on the catenaries is reduced by 75% by decreasing the load current. Additionally, making the system reversible allows for the recovery of unutilised braking energy on the DC grid, which would otherwise be lost as heat, by feeding it back into the AC grid.

2.1 | Upgrading of traction voltage to 3 kV

A DC TS is made up of various components, which can be broadly grouped into four main categories: MV board which includes switchgear and infrastructure on the AC side; traction transformers, diode rectifiers and LV system, which includes equipment such as a LV switchboard, auxiliary transformers, voltage limiters, and control devices. In addition to these major components, various digital and civil infrastructure elements support the overall operations of the substation. The cost of the traction transformers and diode rectifiers can account for up to 23% of the total capital costs of a DC traction substation [23]. With an increase in voltage, the substation's LV side equipment needs to be replaced with newer rated equipment, whereas the MV side equipment can still be reused. If the existing transformer-rectifier groups can be reconfigured, it could result in significant cost savings and a faster transition time. Hence, this paper proposes topologies that can upgrade the substations' DC voltage by reconfiguring the transformer-rectifier groups instead of changing them for new ones.

The configuration shown in Figure 2 is proposed for three-winding transformer-based DC TSs, where a 3 kV output is achieved by changing the internal configuration of each 12-pulse parallel rectifier into the 12-pulse series rectifier. For the case of two-winding transformer-based substations, the two 6-pulse parallel rectifier groups can be connected in series to achieve a 12-pulse 3 kV DC output as shown in Figure 3.

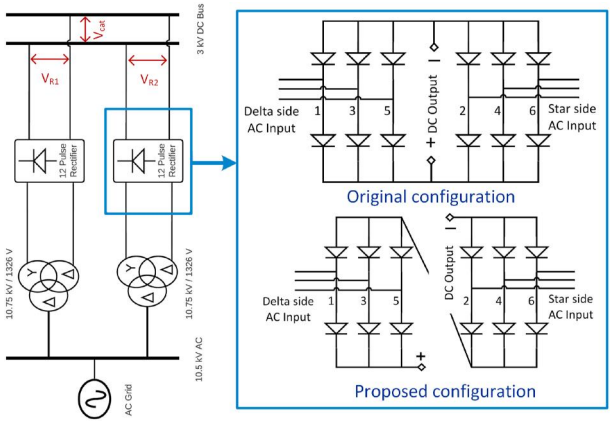

FIGURE 2 Stepping up of voltage by reconfiguring 12-pulse parallel rectifier into 12-pulse series rectifier for DC traction substations (TS) with a three-winding transformer.

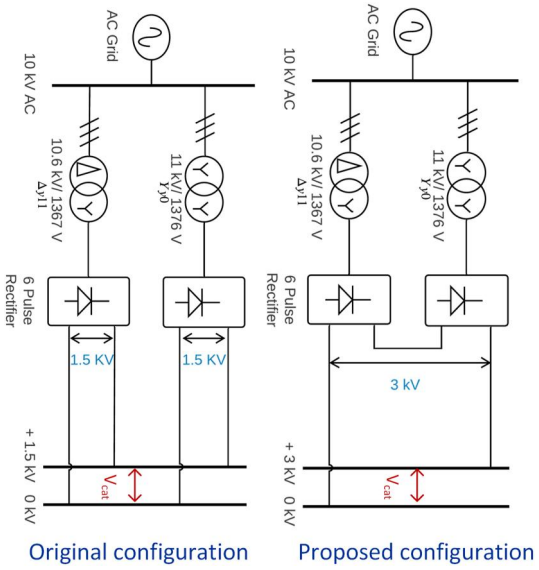

FIGURE 3 Stepping up of voltage by reconfiguring 6-pulse parallel rectifiers output for DC traction substations (TS) with a two-winding transformer.

Both proposed topologies use the modularity of individual 6-pulse rectifiers, potentially saving capital costs and expediting the transition.

2.2 | Topologies for converting uni-directional substations into reversible substations

Reversible energy flow is achieved through parallel VSC operated in inverter mode. The main advantages of parallel VSCs include minimal modification of the current system, which helps save high-cost equipment like rectifiers and transformers. As shown in Figure 4, the parallel inverters can be attached in several arrangements. Options 1–3 uses the existing rectifier

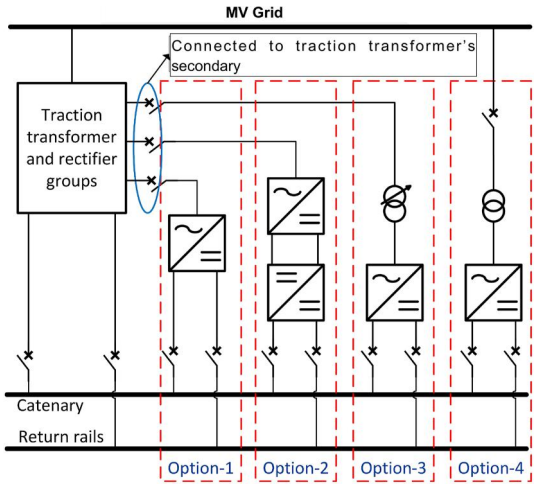

FIGURE 4 Different options for connecting voltage source converters (VSCs) in parallel with the diode rectifiers.

transformers' secondary winding. Option-2 uses a DC-DC converter on the DC side of the VSC, while Option-3 uses an auto-transformer on the AC side of the VSC to better correlate the voltage levels between DC and AC sides. In contrast, these arrangements do not need an additional transformer to connect with the grid but use complex control systems. To keep the VSCs independent of the existing network, which allows isolating it when required (for maintenance/faults), the authors propose Option-4, which uses a dedicated transformer to directly connect with the MV grid. Moreover, an independent transformer can also help evacuate DRES' power into the utility grid, offering better controllability of parallel VSCs in inverter mode. Using a $\Delta - Y_g$ configuration, the number of turns in the primary can be reduced, hence the cost. Also, the delta winding prevents the leakage of zero sequence current into the utility grid, while grounded secondary star winding quickly detects asymmetrical faults.

The VSC's ratings can be much smaller than that of the actual DC TS, as the sizing of the VSC only depends on the maximum braking energy available at any given time. As the reuse of braking energy is given a higher priority, the excess braking energy in the DC grid is always less than the substation's capacity. This will enable us to customise the VSCs size for each DC TS based on historical loading values and save installation costs. For example, a regenerative inverter of only 1.5 MVA must be installed in a DC TS with a 4.8 MVA, covering a 12 km double-track section used by approximately nine trains per hour [24]. This shows that the capacity of parallel VSCs needs to be 30% of the TS's capacity. To use the operational versatility of the VSCs to make the DC TS flexible, different operational modes are modelled and tested as shown in Table 2.

Proper correlation between an inverter's AC and DC side voltages must be done to ensure proper functioning. Especially with PWM inverters, the DC side voltage needs to be above a certain threshold for pushing DC power into the AC grid. Calculations explaining this aspect in detail can be found in Appendix A.

TABLE 2 Modes of operation for voltage source converter (VSC).

Operational modes		Trigger	Control strategy
Inversion	DC energy recuperation	(Automatically) when $V_{DC} > V_{DC}^{nom}$	Decoupled current based control
	Var compensator	Explicit request from DSOs	
	AC voltage support	Only in case of weak MV grid	
Rectification		(Manually) when fault detected in diode rectifier groups	Hysteresis current control
Active power filtration		Manually only in case of 6-pulse diode rectifiers	Control using instantaneous reactive power

3 | MODELLING OF COMPONENTS

3.1 | Modelling of DC traction network

A part of the DC traction network is modelled using two DC TS connected through a single line, travelled by a single train. Electrically the two substation model can be represented by a fixed DC voltage source representing diode-rectifier groups, DC current sources (VSCs operating in inverter mode), DC voltage source (VSCs operating in rectification mode), controlled current source representing a train and variable resistances representing tracks and return rails as shown in Figure 5. The equivalent series resistance (R_{eq}) of each DC TS is calculated from the slope of its current (i) v/s voltage (v) droop characteristics equation (cf. EN 50328:2003) as given in Equation (1).

$$v - V_{DC}^{nom} = \frac{U_{d0} - V_{DC}^{nom}}{-I_b}(i - I_b) \tag{1}$$

V_{DC}^{nom} is the nominal voltage, U_{d0} is the no-load voltage, and I_b is the base current calculated assuming a base power of 2 × 5.4 MVA and a nominal voltage of 3 kV.

The train's movement is modelled by utilising an effect-cause modelling technique, which takes the speed profile as an input to the train model. The train's motion consisting of several waggons can be well described by its position $x(t)$, speed $s_t(t)$ and acceleration $a_t(t)$, which can be derived from the forces acting on the train using Newton's second law of motion [25]. The correlation between the train's current and forces acting on it is done using Equations (2)–(6), where F_{trac} is the total traction force applied by the train motors responsible for the forward movement of the train, F_{res} is the total resistive force experienced by the train, λ_{gear} is gearbox ratio, τ_a and τ_m are the torques delivered by the axle and motor respectively, I_{trac} is the total current absorbed or supplied (during braking) by the whole train comprising of N waggons, η_{conv} and η_{motor} are the assumed efficiencies of converters and motors respectively. The simulation parameters belong to the Nederlandse Spoorwegen (NS) fleet's VIRM-VI class train. Electrically, the train is simulated as a controlled current source, whose current magnitude is calculated from the speed profile using the flowchart of Figure 6b.

$$F_{trac}(t) - F_{res}(t) = M_t \frac{d(s_t(t))}{dt} \tag{2}$$

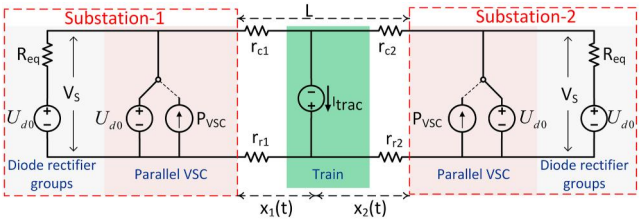

FIGURE 5 Schematic of the electrical equivalent model for the two DC traction substations (TS) model used for simulation. The two substations are connected through a single track used by a single train, where I_{trac} represents a train load.

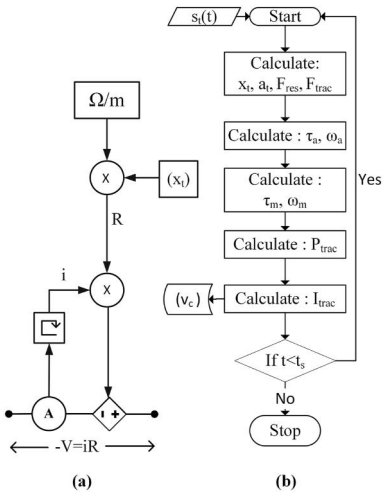

FIGURE 6 (a) Equivalent electrical circuit for calculating catenary and rail resistances. (b) Flowchart for the calculation of the train's output current.

$$F_{res}(t) = C_1 M_{res} + C_2 M_{res} s_t(t) + C_3 N s_t(t) + (C_4 + NC_5) s_t^2(t) \tag{3}$$

$$\tau_a(t) = r_t F_{trac}(t) \quad \text{and} \quad \omega_a(t) = \frac{s_t(t)}{r_t}\frac{60}{2\pi} \tag{4}$$

$$\tau_m(t) = \begin{cases} \dfrac{\tau_a}{\lambda_{gear}} + \dfrac{\tau_a\left(1-\eta_{gear}\right)}{\lambda_{gear}}; & \forall\ \dfrac{ds_t(t)}{dt} \geq 0 \\ \dfrac{\tau_a}{\lambda_{gear}} - \dfrac{\tau_a\left(1-\eta_{gear}\right)}{\lambda_{gear}}; & \forall\ \dfrac{ds_t(t)}{dt} < 0 \end{cases} \tag{5}$$

$$I_{trac}(t) = \frac{\tau_m(t)\frac{\omega_a(t)}{\lambda_{gear}}}{v_c(t)} * \eta_{conv}\eta_{motor} \quad (6)$$

Modelling of tracks is done using variable resistances modelled as variable voltage sources as shown in Figure 6a [26]. The required voltage is calculated from the train's position $x(t)$ w.r.t a substation. $x_1(t)$ and $x_2(t)$ are calculated using Equations (7) and (8), where t and t_s are the current and end simulation time.

$$x_1(t) = \int_0^t s_t(t)dt \qquad \forall \quad 0 \le t \le t_s \quad (7)$$

$$x_2(t) = L - x_1(t) \quad (8)$$

3.2 | Modelling of voltage source converter

In this paper, two VSCs are connected in parallel per DC TS, each with a capacity of 500 kVA as shown in Figure 7. The power of the VSCs is chosen by assuming the maximum braking energy of a train not to exceed 2 MW between two consecutive substations. A simple LCL filter is selected to interface the VSC with the grid due to its higher filtering capacity, cost-effectiveness and smaller size than other available options. The LCL parameters used in this thesis are tuned, considering the VSC side current ripple and grid side Total Harmonic Distortion (THD) [27]. Control strategies for the various operational modes listed in Table 2 are discussed below. Refer to Figure 7 for the connection schematic and control variables used in this section.

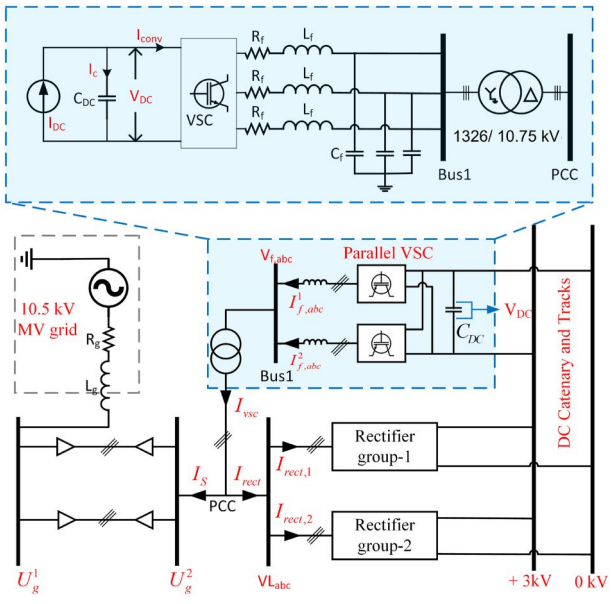

FIGURE 7 Arrangement of parallel voltage source converters (VSCs) in the DC traction substations (TS) and how it is connected to the medium voltage (MV) grid using an LCL filter. The rectifier groups consist of both the rectifier transformer and the diode rectifier.

3.2.1 | Inverter operation

The primary use of parallel VSCs is feeding the excess train's braking energy into the AC grid. The VSCs act as inverters whenever the DC grid voltage exceeds the no-load voltages (U_{d0}). This keeps the DC current minimum, reducing line losses and maintaining the overshoot voltage below 3900 V as specified in EN 50163.

All the VSCs are controlled during inverter operation using an inner and outer loop controller responsible for controlling output current and DC-link voltage, respectively, as shown in Figure 8a. The inner current controller is realised using PI blocks, which help separately control active and reactive current, absorbed/supplied by the VSC using the current reference set-points [28–30]. The voltage controller generates the active current reference (cf. Figure 8a), while the reactive current reference is generated depending on the VSC's submode. A three-phase locked loop (PLL) based on a synchronous frame is used to synchronise all control operations [31]. Equations (9) and (10) shows the closed-loop transfer function of the PLL for a three-phase balanced system used for calculating the gain K_p^{PLL} and K_i^{PLL} of the PI controller.

$$G^{PLL}(s) = \frac{K_{PLL}(s)}{s + K_{PLL}(s) * V_f} \quad (9)$$

$$where: \quad K_{PLL} = K_p^{PLL} + \frac{K_i^{PLL}}{s} \quad (10)$$

Equations (11) and (12) decouples the d and q components of the current using a PI controller having the gains K_p^c and K_i^c respectively.

$$V_d^* = \left[K_p^c + \frac{K_i^c}{s}\right](I_{dref} - I_d) + V_d - \omega L_f I_q \quad (11)$$

$$V_q^* = \left[K_p^c + \frac{K_i^c}{s}\right](I_{qref} - I_q) + V_q - \omega L_f I_d \quad (12)$$

Using the closed loop transfer function of the current controller Equation (13), its denominator $s^2 + \frac{R_f + K_p^c}{L_f}s + \frac{K_i^c}{L_f} = 0$ is compared with the characteristic second order equation $s^2 + 2\zeta^c\omega_n^c s + (\omega_n^c)^2$, to get the desired gains as given in Equation (14). The gains depend on the current controller's performance parameters such as percentage overshoot $\left(M_p^c\right)$, damping factor (ζ^c), steady-state error percentage (ϵ^c), natural frequency $\left(\omega_n^c\right)$, and settling time $\left(T_s^c\right)$.

$$G^i(s) = \frac{K_p^c s + K_i^c}{L_f s^2 + \left(R_f + K_p^c\right)s + K_i^c} \quad (13)$$

$$K_p^c = 2\zeta^c\omega_n^c L_f - R_f \qquad \text{and} \qquad K_i^c = L_f(\omega_n^c)^2 \quad (14)$$

Assuming ideal converter switches, the AC and DC side power is equal as given in Equation (15). Equations (16) and (17) show that by regulating the d component of the AC side current of the converter (I_d), the DC voltage (V_{DC}) can be controlled.

$$P_{DC} = P_{AC} \tag{15}$$

$$P_{AC} = V_d^* I_d + V_q^* I_q \quad \text{and} \quad P_{DC} = V_{DC} I_{DC} \tag{16}$$

$$V_d^* I_d = V_{DC} I_{DC}; \quad \text{As } V_q* = 0 \tag{17}$$

Equations (18) and (19) are used to derive the closed loop transfer function for the voltage controller as given in Equation (20), where K_p^v and K_i^v are the proportional and integral gains respectively.

$$I_c = C_{DC} \frac{dV_{DC}}{dt} \tag{18}$$

$$V_{DC}(s) = \frac{1}{sC_{DC}} I_c(s); \quad \text{laplace transformation} \tag{19}$$

$$G^v(s) = \frac{K_p^v s + K_i^v}{C_{DC} s^2 + K_p^v s + K_i^v} \tag{20}$$

$$K_p^v = 2\zeta^v \omega_n^v C_{DC} \tag{21}$$

$$K_i^v = C_{DC} \left(\omega_n^v\right)^2 \tag{22}$$

The outer loop controller should be at least 10 times slower to stabilise the VSC. [32, 33].

VAR compensator mode is activated manually when there is an explicit demand for reactive power by the DSOs. The converters operate in '**mode-2**' (cf. Figure 7) to generate reactive current reference $\left(I_{qref}^{1,2}\right)$. The DC voltage controller calculates the current reference $\left(I_{dref}^{1,2}\right)$. The superscripts on the reference currents refer to the two VSC operating parallelly. The parallel VSC supply an equal amount of active and reactive reference current to make the control system robust and simple. Reference currents ($I_{dref}^{1,2}$ and $I_{qref}^{1,2}$) are calculated using instantaneous reactive power theory as shown in Equation (23), where $V_{f,d}$ and $V_{f,q}$ are the d and q components of the measured bus voltage $V_{f,abc}$ [34].

$$\begin{bmatrix} I_{dref}^{1,2} \\ I_{qref}^{1,2} \end{bmatrix} = \frac{1}{V_{f,d}^2 + V_{f,q}^2} \begin{bmatrix} V_{f,d} & -V_{f,q} \\ V_{f,q} & V_{f,d} \end{bmatrix} \begin{bmatrix} P_{ref} \\ Q_{ref} \end{bmatrix} \tag{23}$$

As in this case, recuperation of regenerative power is of higher priority, $I_{dref}^{1,2}$ is known, and $I_{qref}^{1,2}$ is calculated using matrix manipulation. When there is no explicit demand for reactive power, the reactive reference current is generated using '**mode-3**', where the objective is to maintain the MV grid voltage at the rated value. In all other times, $I_{qref}^{1,2}$ is kept at 0 to make the VSC operate at unity power factor ('**mode-1**').

3.2.2 | Active power filtration mode

The VSCs can actively compensate for the harmonic current used by the traction rectifiers, reducing the THD in the voltage and current at the PCC. The total compensation current from the parallel VSCs (I_{VSC}) is composed of $\left(I_{f,abc}^{1}\right)$ and $\left(I_{f,abc}^{2}\right)$, each compensating the harmonic current consumption of rectifier group-1 and group-2 respectively. In this paper, instantaneous p-q theory is applied to detect the harmonic content from the load current as shown in Figure 8b [35]. Using Equation (24), the abc component of current is transformed into $\alpha\beta$ components, which is then used to calculate the active $\left(I_{L,p}^{1,2}\right)$ and reactive currents $\left(I_{L,q}^{1,2}\right)$ using Equation (25).

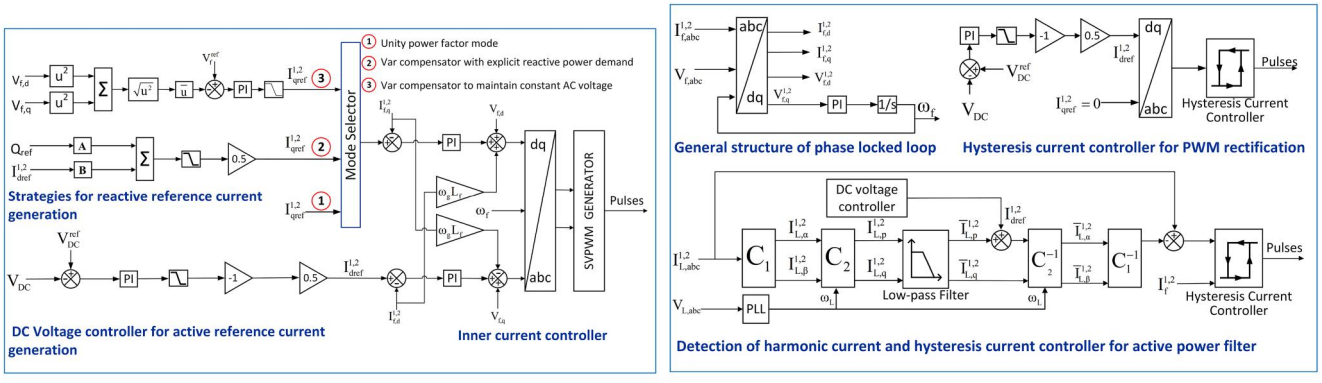

(a) (b)

FIGURE 8 Control schematics used for different modes of operation for parallel voltage source converters (VSCs). (a) Control strategies for the operation of VSC as an inverter. (b) Control strategies for operating VSC as an active power filter (APF) and pulse width modulation (PWM) rectifier.

$$I_{L,\alpha\beta}^{1,2} = \boldsymbol{C_1} I_{L,abc}^{1,2} \quad \text{and} \quad I_{L,abc}^{1,2} = \boldsymbol{C_1^{-1}} I_{L,\alpha\beta}^{1,2}$$
$$\text{where : } \boldsymbol{C_1} = \frac{\sqrt{2}}{3}\begin{bmatrix} 1 & -0.5 & -0.5 \\ 0 & \frac{\sqrt{3}}{2} & -\frac{\sqrt{3}}{2} \end{bmatrix} \tag{24}$$

$$I_{L,pq}^{1,2} = \boldsymbol{C_2} I_{L,\alpha\beta}^{1,2} \quad \text{and} \quad I_{L,\alpha\beta}^{1,2} = \boldsymbol{C_2^{-1}} I_{L,pq}^{1,2}$$
$$\text{where : } \boldsymbol{C_2} = \boldsymbol{C_2^{-1}} = \begin{bmatrix} \sin(\omega_L) & -\cos(\omega_L) \\ -\cos(\omega_L) & -\sin(\omega_L) \end{bmatrix} \tag{25}$$

The active and reactive currents are composed of both the fundamental $\left(\overline{I}_{L,p}^{1,2}, \overline{I}_{L,q}^{1,2}\right)$ and harmonic components $\left(\tilde{I}_{L,p}^{1,2}, \tilde{I}_{L,q}^{1,2}\right)$ as given in Equations (26) and (27), from which the fundamental component is derived by passing the signals through a low-pass filter.

$$I_{L,p}^{1,2} = \overline{I}_{L,p}^{1,2} + \tilde{I}_{L,p}^{1,2} \tag{26}$$

$$I_{L,q}^{1,2} = \overline{I}_{L,q}^{1,2} + \tilde{I}_{L,q}^{1,2} \tag{27}$$

During active filtration mode, the DC link capacitors operate in floating conditions. Hence, an additional amount of current has to be added to the fundamental component of active current to compensate for any loss in the converter and maintain a constant voltage across the capacitors. Once the net fundamental currents are detected, they are transformed back to abc components and subtracted from the total current to obtain only the harmonic part, which is a reference to the hysteresis current controller to generate pulses for the converters.

3.2.3 | Rectification mode

By using the VSCs as PWM rectifiers, the redundancy of DC traction substations can be increased. Primarily this will help avoid downtime during faults in diode-rectifier groups. This paper uses voltage-oriented control of hysteresis band PWM for the converter's pulse generation [36]. However, it should be noted that the operation of VSCs as PWM rectifiers only contributes to a part of the DC traction substation's capacity. During PWM rectification, braking energy recuperation is no longer possible by the same VSCs.

4 | RESULT ANALYSIS

Numerous computer-aided simulations were carried out with the Netherlands' case-specific data to validate the proposed topologies, whose results are presented below.

4.1 | Simulation of a single DC TS in an open loop under no-load conditions

The re-configuration of transformer-rectifier groups to step up the voltage is simulated in Simulink for both two-winding and three-winding-based DC TS. The topologies discussed in Section 2.1 were simulated in Simulink under no-load conditions for a single substation for both two-winding and three-winding substations. Figure 9 illustrates the DC side voltage waveform of the older and proposed configurations for both

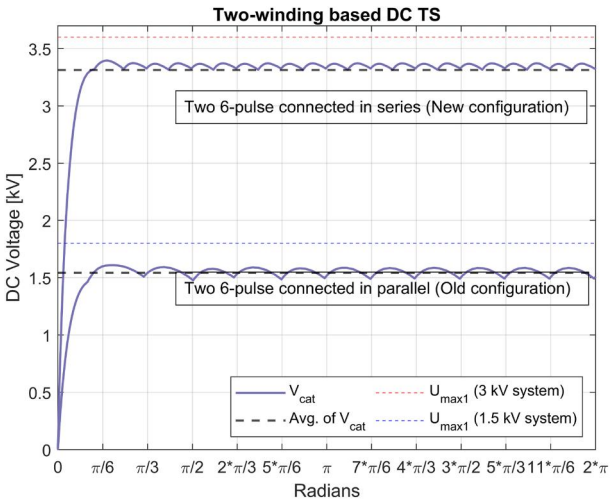

(a)

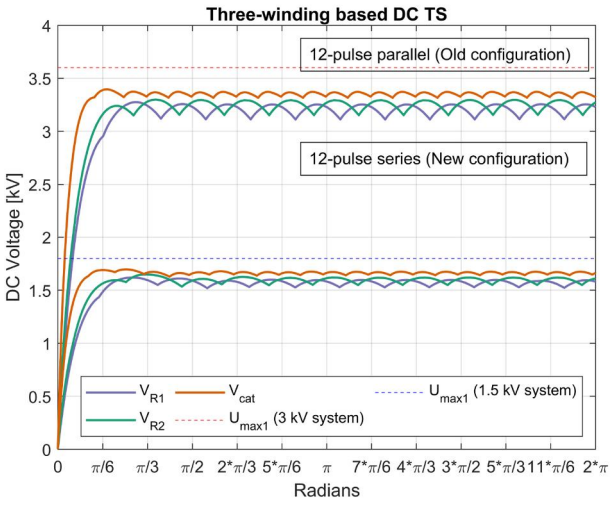

(b)

FIGURE 9 DC voltage waveforms for old and reconfigured diode rectifiers for both types of existing DC traction substations (TS). (a) Results for two-winding transformer-based substations, where the existing 6-pulse rectifier's output is reconfigured from parallel to series connection. (b) Results for three-winding transformer-based substations, where the existing 12-pulse parallel rectifiers are reconfigured into 12-pulse series rectifiers.

types of existing DC substations. The figure shows the DC voltage measured between the catenary and return rails (V_{cat}) as well as the voltage at the terminals of individual 12-pulse diode rectifiers of the three-winding based DC traction substation (V_{R1} and V_{R2}). U_{max1} refers to the allowed highest permanent voltage in the DC network according to the standard: NEN-EN 50163 (Railway applications—Supply voltages of traction systems).

For the re-configured three-winding transformer-based DC TS, the combined output of both the new (12-pulse series) and the old (12-pulse parallel) configuration is a 24-pulsed DC. In the case of a two-winding transformer-based substation, the new configuration produces a 24-pulsed DC output in contrast to the 12-pulsed DC output produced by the original configuration. These extra pulses will inherently decrease the harmonic content on the DC side. It is important to note that in the case of a two-winding transformer-based configuration, the series connection of diode rectifiers reduces the redundancy of the TS. However, with parallel VSC's ability to operate as a rectifier (cf. Section 4.2), the original redundancy can still be achieved.

4.2 | Software-in-the-loop simulation of two substation model

The functionalities of DC TS with parallel VSC are validated using scenario-based simulations considering a two-substation model (cf. Figure 10), with the help of OPAL-RT software-in-the-loop simulator. A real-time simulator is essential to conduct long time-period simulations and assess the functionality of the controllers in real-time. Analysis in this subsection is conducted only for three-winding transformer-based DC TSs with the re-configured 12-pulse series rectifiers. Each substation shown in Figure 10 contains two groups of three-winding transformers and 12-pulse series rectifiers, and two parallel converters. Both parallel converters have identical capacities enough to cater for a load of a single Verlengd Inter-Regio Materieel class train, which is a series of six electric multiple-unit double-deck compartments. The arrangement of components in each substation for the two substation model is shown in Figure 7.

4.3 | Normal operating conditions

To validate the proper functioning of the two-substation model of the Netherlands' traction network, first, the model is simulated in real-time for 470 s covering the acceleration, coasting and braking operating regime of a single train journey from one substation to another as shown in Figure 11. The DC power supplied by substation-1 is initially higher due to the proximity of the train. Later, when the train is equidistant from both substations, the two rectifier groups of these TS supply equal power.

In reality, one or more trains could travel on a multi-track section powered by a DC traction substation. To simulate this situation, a realistic loading profile comprising of voltage (V_{data}) and current (I_{data}) values from one of the existing 1.5 kV DC TS of the Dutch TPS is used. The current profile is generated from these values by normalising them to 3 kV and assuming the same power levels. The generated current profile is used as an input of the controlled current source (I_{trac}) behaving as a load to simulate the experimental setup shown in Figure 12. The single substation model was able to maintain the catenary voltage (V_{cat}) for the realistic load profile for the entire duration, as shown in Figure 13. During the period of negative load ($P_{trac} < 0$), energy will be transferred from the DC to the AC grid, which denotes excessive energy in the DC grid due to more trains braking. During this period, parallel VSCs are activated for energy recuperation back to the AC grid.

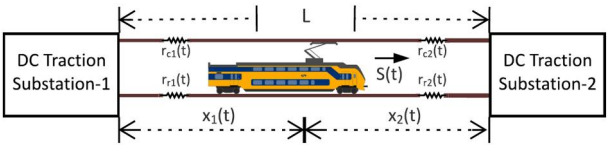

FIGURE 10 Two substation model connected with single-track used for simulation of the upgraded DC traction substations with parallel voltage source converters (VSCs).

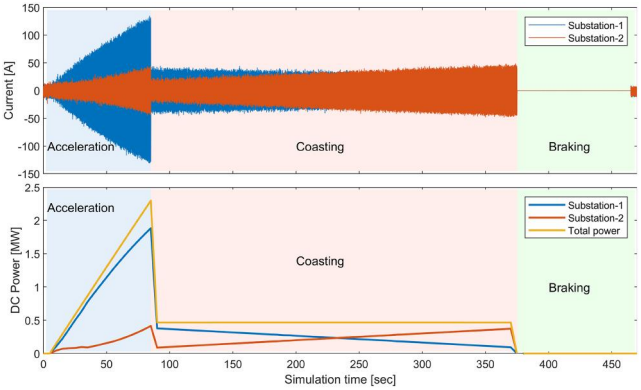

FIGURE 11 AC current supplied by the diode-rectifier groups of both substations (above). The same diode-rectifiers supply DC power in the traction substations (below).

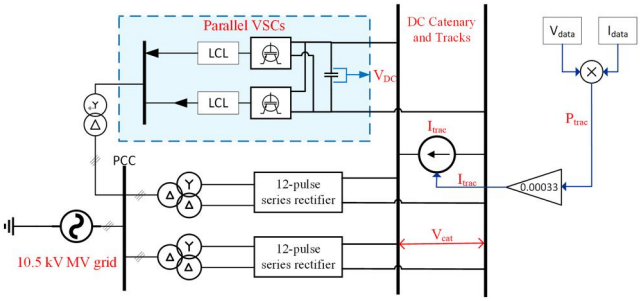

FIGURE 12 Experimental setup to validate the functionality of proposed substations with actual loading levels.

4.4 | VSC as VAR compensator

When few or no trains are braking, the capacity of the VSCs can supply or absorb reactive power from the MV grid. In addition, the extensive controllability of the PWM converters can enable the train operators to support the grid operators during voltage sag and swell in case of a weak MV grid. Figure 14 shows the joint output power of the VSC of a single TS when operated in the 'Q-V_{DC}' control mode. This simulation makes the MV grid less stiff by reducing its short-circuit capacity and the X/R ratio. The MV grid voltages are plotted as dq components per unit. During this scenario, the active power is kept at 0, assuming no train braking.

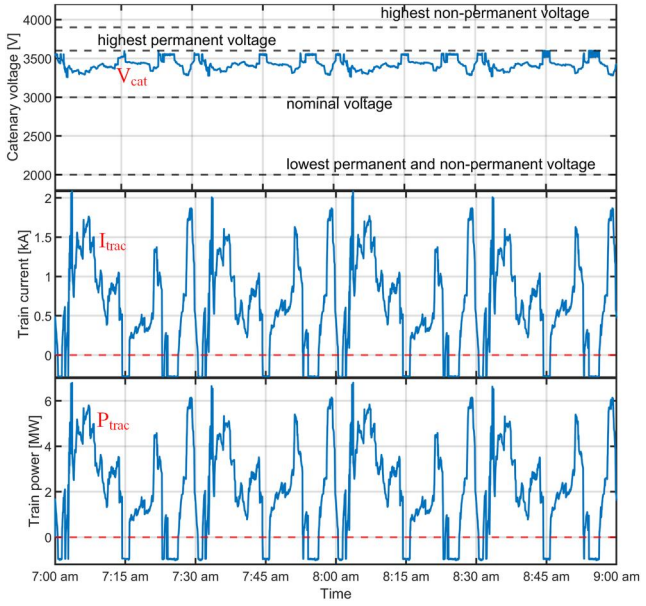

FIGURE 13 Simulation results for a single substation model according to experimental setup of Figure 12 with actual current measurements from existing 1.5 kV substations, normalised for 3 kV voltage level.

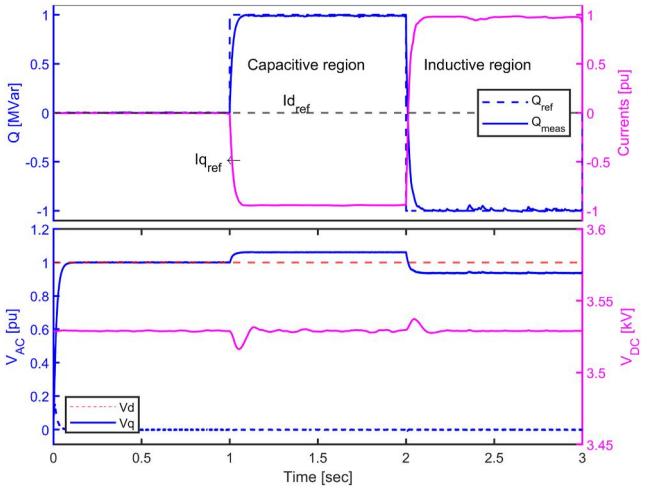

FIGURE 14 Variation of the reactive power output of voltage source converter (VSC) based on varying references (above). Effect of VSC's reactive power absorption/consumption on the AC grid voltage (below).

4.5 | Active power filtration

DC traction substations are highly susceptible to harmonic distortion due to considerable variation in loading levels, voltage unbalance, or non-linear loads [35, 37]. To keep the THD of the MV grid's voltage and current within permissible limits (as per IEC 61000), the current DC traction substations employ two groups of parallel rectifiers (12-pulse or 6-pulse) separated mutually by a phase difference of 15°, which gives an output of either 12-pulse or 24-pulse DC respectively [38]. 24-pulse output requires two three-winding transformers, and 12-pulse output requires two two-winding transformers, incurring additional cost and maintenance. On the other hand, a 6-pulse rectified output is the most cost-effective arrangement but has a considerable amount of 3rd and 5th harmonics compared to 12 or 24-pulse rectifiers.

Shunt VSCs can operate as Active Power Filters (APFs) and compensate for the load's harmonic current. Hence to test the effectiveness of active power filtration capabilities of the proposed VSCs, a single DC TS containing two groups of 6-pulse rectifiers is equipped with a set of parallel VSCs operating as APF. The setup is simulated for 10 cycles with a load current of $0.5I_{base}$ for the first cycles and then increased to I_{base} for the last five cycles. Figure 15 shows the load (I_{load}), source (I_S) and harmonic compensation (I_{VSC}) currents. I_{load} consists of both the fundamental and harmonic components, whereas the compensated currents provided by the APF only contain the harmonic currents. As a result, the current drawn from the source has a very low THD, shown in the FFT analysis of all the three current waveforms (Figure 15). The negative magnitude of the VSC current's magnitude in the FFT analysis is only for visualisation purposes. It can also be seen that the active filter adapts itself to changing loads within one cycle.

4.6 | PWM rectification and inclusion of RES

One of the significant advantages of the bi-directional 3 kV system is including DRES directly in the DC grid. A RES unit modelled as a controlled current source is connected to the two-substation model for this case. The whole simulation is then divided into three regions. In region-1, all the rectifier groups of both substations are active, and the power consumption of the train is more than that of the power generated by the RES; hence the diode-rectifiers supply DC power to the DC grid as shown in Figure 16. During region-2, one of the rectifier groups of substation-1 is shut down due to maintenance. Detecting the failure in the diode-rectifier, the VSCs of substation-1 start operating as a PWM rectifier and supply the required DC power to the train as shown in Figure 16. The last region shows the transformation of the VSCs in both substations from ideal or PWM rectification modes into inverter

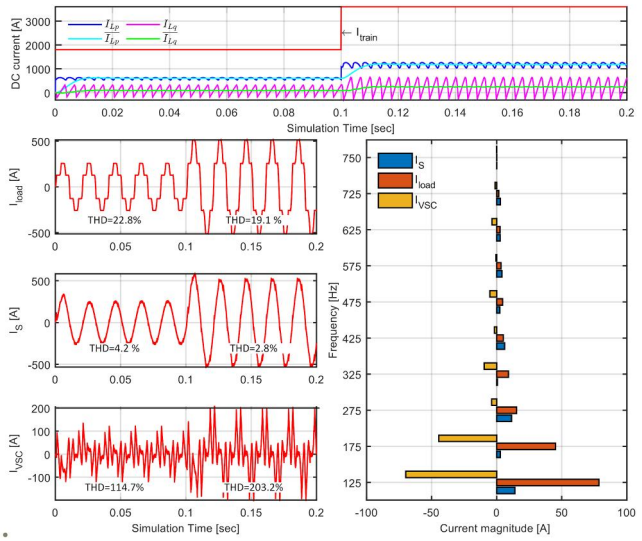

FIGURE 15 Effect of variation in load current on the active power filter (APF) and fast-Fourier analysis of source, load, and active filter current.

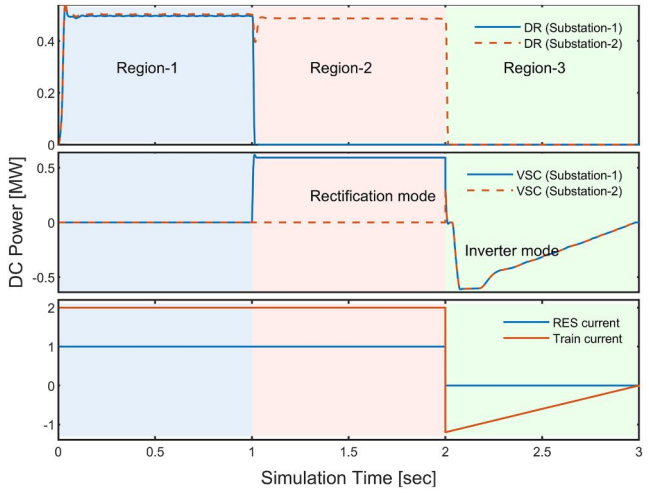

FIGURE 16 Variation of DC power output of rectifiers, voltage source converters (VSCs), train and RES.

operating modes. This region is triggered by the loss of RES power and braking of the train leading to a rise in DC grid voltage.

5 | CONCLUSION

This paper presents innovative methods and topologies for upgrading 1.5 kV unidirectional DC traction substations in the Netherlands' railway network into 3 kV efficient and bi-directional substations using power electronics. The proposed approach offers practical solutions for stepping up the system voltage from 1.5 to 3 kV by modifying existing equipment instead of replacing it completely. The two proposed topologies cater to two-winding and three-winding transformer-based substations and meet EN standards while satisfying the operating requirements of the Dutch railways. The upgraded designs not only raise the voltage of the traction power supply but also integrate parallel VSCs, making the existing DC traction substations reversible. This improves traction power supply efficiency by recuperating braking energy that would otherwise be lost as heat and reduces catenary losses through higher voltage and lower load current. The paper underscores the significance of electrified public transportation networks, the need to modernise older and less efficient traction power networks for more efficient public transportation, and possible support to the utility grid. The proposed topologies not only improve the electrical efficiency (reducing copper losses) but also enhance the non-electrical efficiency of the system, resulting in faster acceleration and deceleration of locomotives and aiding in the maintenance of a busy train schedule. The suggested use cases of VSC's functionalities, like reactive power compensation and aiding the integration of DRESs, will not only add new revenue streams to the railway operators but also aid in the energy transition by supporting the utility grid.

This study presents a unique and practical solution tailored to the traction power networks in the Netherlands. It advocates a cost-effective strategy that leverages existing substation equipment, an under-represented aspect in academic literature. Transforming the Netherlands' 1.5 kV traction network into a 3 kV bi-directional and controllable traction network is a crucial long-term objective for its stakeholders. The paper compares the efficiency and cost-effectiveness of various solutions from the current literature and recommends the most optimal approach. It is imperative to note that additional research on digital and civil infrastructure compatibility with the 3 kV voltage level solution is essential before embarking on the actual transition.

AUTHOR CONTRIBUTIONS

Nanda Kishor Panda: Conceptualisation; Data curation; Formal analysis; Investigation; Methodology; Validation; Visualisation; Writing—original draft. **Michail Poikilidis**: Methodology; Project administration; Resources; Supervision; Writing—review & editing. **Phuong H. Nguyen**: Supervision; Writing—review & editing.

ACKNOWLEDGEMENTS

This work was performed in collaboration with DNV Energy, Arnhem, The Netherlands and the Eindhoven University of Technology, The Netherlands, under the innovation project framework. The authors thank ProRail- part of NS Railinfratrust, the Dutch railway infrastructure owner, for providing data and insights related to this work. The work leading to this paper is part of the FlexiGrid project (https://flexigrid.org/), which received funding from the European Union's Horizon 2020 research and innovation programme under Grant Agreement No. 864048.

CONFLICT OF INTEREST STATEMENT

We have no conflict of interest to disclose.

DATA AVAILABILITY STATEMENT

The data that support the findings of this study are available from DNV. Restrictions apply to the availability of these data, which were used under license for this study. Data are available from the authors with the permission of DNV.

ORCID

Nanda Kishor Panda https://orcid.org/0000-0002-9647-4424

Phuong H. Nguyen https://orcid.org/0000-0003-1124-2710

REFERENCES

1. Verdicchio, A., et al.: New medium-voltage DC railway electrification system. IEEE Trans. Transport. Electrification 4(2), 591–604 (2018). https://doi.org/10.1109/tte.2018.2826780
2. Zoeteman, A.: Analysing the business case for introducing a 3 kV traction power supply in Dutch railways. In: ten Harve, F., Ploeg, T. (eds.) WIT Transactions on the Built Environment, vol. 135, pp. 745–755 (2014)
3. Dielesen, J.: ACM Rail Monitor: the Netherlands Has Europe's Busiest Railway Network – ACM.nl. Authority for Consumers & Markets (2019). https://www.acm.nl/en/publications/acm-rail-monitor-netherlands-has-europes-busiest-railway-network
4. A social cost-benefit analysis of an improved traction energy supply: elaboration of the alternatives 3kV and 1.5kV ECO', NS and Prorail. Tech. Rep., (2018). https://www.eerstekamer.nl/overig/20180622/een_maatschappelijke_kosten_baten/document
5. Reijnen, D.: The Contribution of 3kV DC Traction Power Supply System to Railway Capacity in the Netherlands (MSc Thesis). Delft University of Technology (2017)
6. Gelman, V.: Harmonics effect on rectifier current imbalance. In: 2004 11th International Conference on Harmonics and Quality of Power, pp. 789–793. IEEE (2004)
7. Kulesz, B.: Rectifier transformers in electric traction substations-Different designs. Transport 20(2), 66–72 (2005). https://doi.org/10.3846/16484142.2005.9637998
8. European standards: NEK EN 50328:2003 for Railway applications - fixed installations, Norwegian electrotechnical standard (NEN). Tech. Rep., (2003). https://standards.iteh.ai/catalog/standards/sist/1ce98ecd-df10-4250-9196-64d9b034ea98/sist-en-50328-2004
9. Tian, Z., et al.: Energy evaluation of the power network of a DC railway system with regenerating trains. IET Electr. Syst. Transp. 6(2), 41–49 (2016). https://doi.org/10.1049/iet-est.2015.0025
10. Everett, A.: Electric railway traction. J. Inst. Eng. Electron. 57(2S), 312–316 (1919). https://doi.org/10.1049/jiee-1.1919.0078
11. Aeberhard, M., Courtois, C., Ladoux, P.: Railway traction power supply from the state of the art to future trends. In: SPEEDAM 2010, vol. 6, pp. 1350–1355. IEEE (2010)
12. Bałkowiec, T.: Three-phase rectifier dedicated to DC traction substation. Przeglad Elektrotechniczny 1(9), 43–47 (2017). https://doi.org/10.15199/48.2017.09.08
13. Sikora, A., Kulesz, B.: Effectiveness of different designs of 12- and 24-pulse rectifier transformers. In: 2008 18th International Conference on Electrical Machines, vol. 9, pp. 1–5. IEEE (2008)
14. Sikora, A., Kulesz, B.: Properties of novel traction polyphase rectifier transformer. In: 2012 XXth International Conference on Electrical Machines, vol. 2, pp. 2139–2144. IEEE (2012)
15. Szymanski, J.R., et al.: Simulation research of low-voltage modules of rectifier in 3kV railway substation. In: 2020 IEEE First International Conference on Smart Technologies for Power, Energy and Control (STPEC), vol. 9, pp. 1–5. IEEE (2020)
16. Djeghader, Y., et al.: Study and filtering of harmonics in a DC electrified railway system. In: 2015 7th International Conference on Modelling, Identification and Control (ICMIC), No. ICMIC, vol. 12, pp. 1–6. IEEE (2015)
17. Popescu, M., Bitoleanu, A.: A review of the energy efficiency improvement in DC railway systems. Energies 12(6), 1092 (2019). https://doi.org/10.3390/en12061092
18. Gelman, V.: Energy savings with reversible thyristor controlled rectifier. In: 2009 Joint Rail Conference, vol. 1, pp. 41–46. ASMEDC (2009)
19. Gelman, V.: Insulated-gate bipolar transistor rectifiers: why they are not used in traction power substations. IEEE Veh. Technol. Mag. 9(3), 86–93 (2014). https://doi.org/10.1109/mvt.2014.2333762
20. Wang, L., et al.: A Novel traction supply system for urban rail transportation with bidirectional power flow and based on PWM rectifier. In: 2009 International Conference on Energy and Environment Technology, vol. 2, pp. 40–43. IEEE (2009)
21. González-Gil, A., Palacin, R., Batty, P.: Sustainable urban rail systems: strategies and technologies for optimal management of regenerative braking energy. Energy Convers. Manag. 75, 374–388 (2013). https://doi.org/10.1016/j.enconman.2013.06.039
22. Khodaparastan, M., Mohamed, A.A., Brandauer, W.: Recuperation of regenerative braking energy in electric rail transit systems. IEEE Trans. Intell. Transport. Syst. 20(8), 2831–2847 (2018). https://doi.org/10.1109/tits.2018.2886809
23. Octávio, M.: DC Traction System Cost Estimation Tool Taking into Account Losses Minimization. Ph.D. dissertation. Universidade NOVA de Lisboa (2020)
24. Bae, C.H., et al.: A study of capacity calculation of regenerative inverter for 1500V DC traction system. WIT Trans. Built Environ. 88(June), 757–766 (2006)
25. Schmid, F., Goodman, C.J., Watson, C.: "Overview of electric railway systems," 7th IET Professional Development Course on Railway Electrification Infrastructure and Systems (REIS 2015), vol. 2015, pp. 1–15. https://doi.org/10.1049/ic.2015.0320
26. Zhao, G., Wei, M., Yang, Z.: Modeling and simulation of regenerative braking of electric bus in antilock braking system. Nanjing Hangkong Hangtian Daxue Xuebao/J. Nan. Univ. Aeronaut. Astronaut. 42(2), 256–261 (2010)
27. Saïd-Romdhane, M.B., et al.: Simple and systematic LCL filter design for three-phase grid-connected power converters. Math. Comput. Simulat. 130, 181–193 (2016). https://doi.org/10.1016/j.matcom.2015.09.011
28. Yazdani, A., Iravani, R.: Voltage-Sourced Converters in Power Systems (2010)
29. Choi, J.-C., et al.: Voltage control scheme with distributed generation and grid connected converter in a DC microgrid. Energies 7(10), 6477–6491 (2014). https://doi.org/10.3390/en7106477
30. Popescu, M., Bitoleanu, A.: Simulink library for reference current generation in active DC traction substations. Int. J. Elect., Comput., Energetic, Electron. Commun. Eng. 9(8), 794–801 (2015)
31. Abbas, S.Z.: Implementation and Testing of Three-phase Controlled Power Inverter Behaviour. Ph.D. dissertation. Universitat Politècnica de Catalunya Escola Tècnica Superior d ' Enginyeria Industrial de Barcelona (2016)
32. Rodriguez, P., Rouzbehi, K.: Multi-terminal DC grids: challenges and prospects. J. Mod. Power Syst. Clean Energy 5(4), 515–523 (2017). https://doi.org/10.1007/s40565-017-0305-0
33. Teodorescu, R., Liserre, M., Rodríguez, P.: Grid Converters for Photovoltaic and Wind Power Systems. John Wiley and Sons, Ltd, Chichester (2011)
34. Herrera, R., Salmeron, P.: Instantaneous reactive power theory: a reference in the nonlinear loads compensation. IEEE Trans. Ind. Electron. 56(6), 2015–2022 (2009). https://doi.org/10.1109/tie.2009.2014749
35. Popescu, M., et al.: Increasing power quality in a 6-pulse DC-traction substation. In: 2017 International Conference on Electromechanical and Power Systems (SIELMEN), vol. 10, pp. 483–488. IEEE (2017)
36. Jamma, M., et al.: Voltage oriented control of three-phase PWM rectifier using space vector modulation and input output feedback linearization

theory. In: 2016 8th International Conference on Electronics, Computers and Artificial Intelligence (ECAI), vol. 6, pp. 1–8. IEEE (2016)
37. Ramos, G., et al.: Instantaneous p-q theory for harmonic compensation with active power filter in DC traction systems. In: 2011 International Conference on Power Engineering, Energy and Electrical Drives, vol. 5, pp. 1–5. IEEE (2011)
38. Singh, B., et al.: Multipulse AC–DC converters for improving power quality: a review. IEEE Trans. Power Electron. 23(1), 260–281 (2008). https://doi.org/10.1109/tpel.2007.911880

How to cite this article: Panda, N.K., Poikilidis, M., Nguyen, P.H.: Cost-effective upgrade of the Dutch traction power network: moving to Bi-directional and controllable 3 kV DC substations for improved performance. IET Electr. Syst. Transp. e12084 (2023). https://doi.org/10.1049/els2.12084

APPENDIX A

Correlation between the inverter's DC side voltage and AC side voltage at PCC

This section determines the lower threshold value for the voltage of the DC grid formed by various rectifier configurations to ensure proper operation of the proposed parallel VSCs.

The no-load voltage (U_{DC0}) can be related to its average nominal voltage(U_{DCN}) and the voltage drop across the power supply(converter) unit (ΔU) using Equation (A1).

$$U_{DC0} = U_{DCN} + \Delta U \tag{A1}$$

Equation (A2) expresses the voltage drop ΔU in the percentage of U_{DCN} and is generally between 5% and 10% depending on one of the regulation standards.

$$\delta U[\%] = \frac{\Delta U}{U_{DCN}} * 100 \tag{A2}$$

Using Equations (A1) and (A2), U_{DC0} can be expressed as follows:

$$U_{DC0} = (1 + \delta U) * U_{DCN} \tag{A3}$$

Again U_{DC0} can be related to the AC line r.m.s. voltage values as follows:

$$U_{DC0} = K_r * \sqrt{2} * U_{AC,rms} \tag{A4}$$

where:

$U_{AC,rms}$ is the r.m.s. line-to-line voltage of the AC grid;

K_r is a coefficient depending on the type of rectifier;

$$K_r = \begin{cases} \frac{3}{\pi} = 0.955 \text{ for 12 pulse parallel rectifier} \\ \frac{6}{\pi} = 1.910 \text{ for 12 pulse series rectifier} \end{cases}$$

From Equations (A3) and (A4), the ratio of U_{DCN} and $\sqrt{2}U_{AC,rms}$ can be expressed using an additional variable K_p as shown in Equation (A5).

$$K_p = \frac{U_{DCN}}{\sqrt{2} * U_{AC,rms}} = \frac{K_r}{1 + \delta U} \tag{A5}$$

The values of K_p for 12 pulse parallel and 12 pulse series rectifiers are calculated as 0.87 and 1.84 respectively.